CLM-P 174






United Kingdom Atomic Energy Authority

RESEARCH GROUP

Preprint

# ION CYCLOTRON INSTABILITIES IN THE PHOENIX II EXPERIMENT

W. CALVERT
J. G. CORDEY
G. KUO-PETRAVIC
E. G. MURPHY
M. PETRAVIC
D. R. SWEETMAN
E. THOMPSON

Culham Laboratory
Abingdon Berkshire

1968

UNCLASSIFIED
(Approved for publication)

CLM - P 174

# ION CYCLOTRON INSTABILITIES IN THE PHOENIX II EXPERIMENT

by

W. CALVERT*
J.G. CORDEY
G. KUO-PETRAVIC
E.G. MURPHY
M. PETRAVIC
D.R. SWEETMAN
E. THOMPSON

(Paper presented at Gatlinburg Conference on Open Ended Systems, November 1967)

## ABSTRACT

Recent results from the PHOENIX II neutral injection experiment are described. The plasma density achieved with magnetic well geometry is limited to about $5 \times 10^9$ cm$^{-3}$ by an instability associated with the ion cyclotron frequency and its harmonics. The harmonic number increases with density and a complex line splitting is observed which may be associated with the axial oscillation frequency of the ions. Phase measurements indicate a half wavelength along the length of the plasma, and a much shorter azimuthal wavelength. Strong coupling to the parallel motion of the electrons is indicated by loop aerial signals and energetic electron ejection through the mirrors. The growth times can be less than a microsecond. At the highest densities some considerable spreading of the ion energy occurs. The properties of this instability are compared with the computations of Beasley and Cordey on electrostatic instabilities of the Harris type. The onset densities for the various harmonics, the ratio $k_{\parallel}/k_{\perp}$ and growth rates are in reasonable agreement. Much of the detailed structure remains to be accounted for but it is not unexpected in finite geometry.

Preliminary results on the effect of microwave heating of the electrons are described. Complete suppression of the higher harmonics is observed but an instability appears at the fundamental of the ion gyro-frequency. There is evidence for reversal of plasma potential resulting in a considerable cold ion component to the plasma and consequently enhanced fast ion trapping. The preliminary results indicate that a fast ion density of about $10^{10}$ cm$^{-3}$ with a comparable cold ion density has been achieved.

*On leave from ESSA, Boulder, Colorado.

U.K.A.E.A. Research Group,
Culham Laboratory,
Abingdon,
Berks.

April, 1968 (MEJ)

CONTENTS

## 1. EXPERIMENTAL OBSERVATIONS ON R-F EMISSION

In this paper are described some experiments carried out with the PHOENIX II apparatus at the Culham Laboratory. In this apparatus a magnetic well is created by superposing a quadrupole cusp field on a simple mirror field[1]. Fig.1 shows the vacuum chamber and coil structure. The central magnetic field is variable from 20 kG downwards but for most of the experiments it was held at 12½ kG.

The plasma is produced by ionizing 20 keV hydrogen atoms with the Lorentz electric field they experience in crossing the magnetic field. A density of about $5 \times 10^9$ cm$^{-3}$ is achieved by the balance of this trapping mechanism against charge exchange and instability losses.

Provided the magnetic well geometry is maintained this experiment is stable to the low frequency flute instability[1]. However, at the highest densities there is considerable R-F activity and Fig.2 shows a typical oscillogram of the amplitude of the R-F activity as a function of time. The signals occur in short bursts with a typical duration of 1-5 ms.

The frequency spectrum of the signal from a loop aerial placed on the median plane near the plasma has been measured as a function of density and Fig.3 shows some typical spectra at various densities. These repetitively swept spectra are integrated over one second. At low densities the emission is predominantly in the first harmonic and gradually as the density is raised emission appears at the second harmonic. At yet higher density the emission at the second harmonic becomes dominant and that at the first is reduced in amplitude. At the highest densities the dominant emission is in the third harmonic. The emission at the fourth harmonic is believed to be generated from that at the second harmonic by some form of non-linear plasma phenomenon.

The detailed substructure within a given harmonic is quite complicated. Near threshold a strong splitting of the basic harmonic structure is observed. This splitting may be associated with the ion axial oscillation frequency of 2·7 MHz. If the spectrum is examined on a short time scale, an even finer substructure and a tendency of the frequency to sweep with time has been seen. This paper is not concerned with the details of this structure but with the general properties of the instability.

Measurements of the phase of the R-F signals have been made using electrostatic probes arrayed along the length of the plasma. Fig.4 shows some of the measurements. The amplitude and phase of the signals from the probes is displayed at the bottom of the figure. A minimum in amplitude, and a phase shift of 180$^o$, occurs near the median plane, showing that there is a standing wave with a half wavelength along the plasma. This detailed measurement has been made on the second harmonic but measurements of the relative phase at the ends indicate that the other harmonics are behaving similarly.

Phase correlation measurements to determine the azimuthal wavelength have been attempted. The number of probes available was not sufficient to determine the mode number unambiguously, but the indications are that the wavelengths in the azimuthal direction are of the order of only a few cm. Consequently there is a fairly large ratio of $\lambda_{\parallel}$ to $\lambda_{\perp}$. Also loop aerials placed outside the plasma show that the currents in the plasma are mostly axial.

Associated with this instability there is a loss of electrons along the field lines. Fig.5 shows the correlation of this electron loss with the R-F activity. Bursts of

electrons with energy greater than 50 eV are clearly correlated with the R-F activity.

An estimate of the growth rate of the instabilities in the various harmonics may be made by looking at the R-F wave-form as a function of time and Fig.6 shows an example of the growth of a burst at the second harmonic. These experiments have not yet been completed but in this example, which exponentiates with a 200 ns time constant, the growth rate is $\cdot 02\ \omega_{ci}$.

## 2. COMPARISON WITH THEORETICAL MODEL

The instability clearly involves the ions since the emission occurs at harmonics of the ion cyclotron frequency. The instability also involves the electrons; the phase correlation measurements indicate that there is a finite axial wavelength and also considerable energy is observed to be given to electrons in the parallel direction. These are the requirements of an electrostatic ion cyclotron instability of the type first discussed by Harris[2]. The results are therefore compared with the theory of Beasley and Cordey[3] which takes the Harris type of dispersion relation, but uses the non-Maxwellian ion velocity distribution given by

$$f(v) \propto v_\perp{}^{2j} \exp\left(-\frac{v_\perp^2}{\alpha_\perp^2} - \frac{v_\parallel^2}{\alpha_\parallel^2}\right)$$

where $j$ determines the width of the distribution. The electron distribution is assumed to be Maxwellian.

In Fig.7 the theoretically predicted growth rates as a function of $\omega_{pe}/\omega_{ci}$ are plotted for the first three harmonics of $\omega_{ci}$ for both the convective and absolute modes of propagation. In plotting the convective curves it has been assumed that the ends are perfectly reflecting and this results in a very fast growing standing wave. The growth rate of the absolute instability increases somewhat more gradually from a higher density threshold. The experimental thresholds for the onset of emission in the first three harmonics are indicated by arrows.

Considering that the theory assumes an infinitely long plasma the agreement between it and the experimental results is surprisingly good. The fast growth rates, measured to be of the order of $\cdot 02\ \omega_{ci}$, do tend to favour the convective interpretation but from this evidence alone it would be unwise to conclude that the instability was convective or otherwise.

A further consideration is whether the theoretically computed parallel wavelength of the instability fits into the plasma. Fig.8 shows the theoretical parallel wavelengths as a function of $\omega_{pe}/\omega_{ci}$, and the experimental thresholds. The dashed curves indicate the limits of parallel wavelengths for the absolute instability and the hard lines indicate the limits of parallel wavelength for the convective instability. In plotting these curves $\lambda_\perp$ has been assumed to be a free parameter and the permissible range of $\lambda_\parallel$ has been plotted at each density for the first three harmonics of $\omega_{ci}$. The values of $\alpha_\parallel/\alpha_\perp$ and $j$ are those appropriate to the computed injected plasma distribution. $T_e$ is taken as 30 eV which is somewhat above the injected energy of 10 eV but is probably reasonable when ionization electrons and ion-electron collisions are taken into account. The boundaries are not sensitive to assumptions of the magnitude of $T_e$ below 100 eV. The hatched horizontal line shows an estimate of the restriction imposed by the actual plasma length.

It is quite difficult to fit the parallel wavelengths for the first harmonic into the finite length plasma but just about possible for the case of the second and third harmonics if the instability is assumed to be convective. However, recent considerations show that the finite geometry increases the effective anisotropy and this reduces the theoretical parallel wavelength and density thresholds somewhat. With this in mind it would be ill-considered to distinguish between convective and absolute instabilities; the distinction is in any case rather academic in a short plasma with highly reflecting ends.

The general conclusion to be reached from these curves is that, as the density is raised, there should be a sudden onset of the instability at a given harmonic, followed by a gradual decline (due to the difficulty of fitting the longer parallel wavelength into the plasma) and that this behaviour should progress to the higher harmonics. This general behaviour is in very good agreement with the experimental results as can be seen from Fig.9 which shows in more detail how the R-F activity behaves as a function of density. Here can be seen the amplitude of the signal from a probe, electrostatically coupled to the plasma, which has been filtered to separate the various harmonics, rectified and integrated over 1 second, plotted as a function of $\omega_{pe}/\omega_{ci}$. As the density is raised the activity in the first harmonic increases and then falls off slowly, but has rather low amplitude at all times; the intensity in the second harmonic comes in at a higher density and reaches a maximum and then falls off, and the intensity in the third harmonic does much the same, increases rather sharply and shows signs of reaching a maximum.

## 3. PARTICLE LOSSES AND ENERGY SPREAD

Fig.10 shows the particle density in the machine as a function of the neutral beam current multiplied by the time constant. The plasma density is determined from the slow ion current through the mirrors which essentially integrates the density along the flux tube centred on the axis. On the basis of Lorentz trapping and loss by charge exchange, the broken line at $45^{o}$ would be expected. At very low densities the experimental results follow this line. At somewhat higher density they rise slightly, probably due to plasma trapping[1]. At higher density they drop sharply below the line and this correlates with the onset of second harmonic emission. As $I_o\tau$ is further increased, the second harmonic emission reaches a maximum and then falls off, the density starts to rise again until the third harmonic threshold is reached when the density again shows signs of saturation.

It is worth noting that the data for this and successive curves was taken by keeping the neutral beam $(I_o)$ approximately constant and varying the gas pressure and hence charge exchange loss time $(\tau)$. If the instability loss is expressed as a 'diffusion time' then this has minima when the second and third harmonic emissions are maximum. These two minimum values are both equal to 200 ms (which in turn corresponds to $10^3$ Bohm times). If this diffusion time proves to be independent of $I_o$ as well as harmonic number it may be possible to increase the density by increasing $I_o$.

The density may be determined another way by looking at the total fast neutral emission from the plasma which is proportional to the product of the fast ion density and the background neutral density. The total neutral emission is measured with a fluorescent screen coupled to a photomultiplier with a light guide. Computations show that this responds to emission from all regions of space containing plasma, though the sensitivity is

not completely uniform. Fig.11 shows that this deviates in much the same way that the line density along the axis deviates from the $45^{o}$ line. This average density does not rise above the $45^{o}$ line, indicating that the plasma trapping is localised to a small volume in the centre.

Collimated fast atom detectors which look at specific regions of the plasma show somewhat more complicated behaviour. Fig.12 shows the neutral emission from the centre of the plasma as measured by one of these collimated detectors. As $I_0\tau$ is raised this emission rises first of all above the $45^{o}$ line and then at the highest density starts to saturate. The rise is believed to be due to the plasma trapping occurring in the centre of the device and in this local region of space the enhanced trapping appears to exceed the instability losses up to a density of $6 \times 10^{9}$ $cm^{-3}$.

The energy spectrum of the neutral atoms emitted near the median plane has been measured using solid state detectors, and several of these energy spectra taken at different densities can be seen in Fig.13. At the top is shown the energy spectrum for a stable pulse at very low density; most of the width in this case is instrumental. As the density is raised the energy spectrum broadens. The middle spectrum is typical of that during second harmonic emission and the lower spectrum typical of that during third harmonic emission. Displays of the energy spectrum as a function of time show good time correlation between R-F bursts and energy spreading.

Fig.14 shows the width of these energy spectra as a function of the density. The width for very stable conditions may be narrower than is indicated here because of the difficulty of measuring widths smaller than the instrumental resolution.

## 4. APPLIED ENERGY SPREADING AND MICROWAVE HEATING

A test of the assignment of a velocity space instability is to vary the ion and electron distribution functions.

Experiments on ion energy spreading have been carried out by applying stochastic heating to the ions while they are in the machine. This method was used with some success to distinguish between ion cyclotron instabilities in simple mirror geometry[4]. These experiments have been repeated with the instability present in well geometry where the behaviour when stochastic heating is applied is found to be complicated and in different regimes both suppression and stimulation of emission have been observed. The effects are believed to be associated with transit-time heating of the electrons rather than ion energy spreading. At this stage in the experimental programme the only conclusion that can be reached is that the instability is still present even with an imposed energy spread in excess of that produced by the instability. Thus energy spreading does not appear to be decisive in eliminating the instability as it was for the $\theta$-mode instability in simple mirror geometry[4].

This behaviour is in good agreement with the infinite geometry theory which predicts in this region little change of either threshold or parallel wavelength with energy spread. Two sample theoretical curves corresponding to different energy spreads are illustrated in Fig.7 for the case of the third harmonic (j = 47 corresponds to a 27% FWHM and j = 11 corresponds to 70% FWHM). However, recent calculations suggest that finite geometry effects may make the instability more sensitive to ion energy spread than the infinite geometry treatment suggests.

A more conclusive experiment has recently been carried out by changing the electron temperature using microwave heating. 8 mm microwaves were used which resonated with the electron gyro-frequency at 11·4 kG. Two distinct regimes were observed.

If the resonant zone is arranged to be about 10% above the bottom of the well, then application of the microwave power completely quenches the emission in the second and third harmonics. However, strong emission appears at the first harmonic. This first harmonic emission is much more continuous and intense than that which was seen at lower densities without microwave heating, and causes an ion energy spread of some 80% FWHM. The particle losses associated with this first harmonic emission are comparable with those associated with the second and third harmonic emission in the absence of microwave heating.

If the resonance zone is arranged to be at the minimum of the well, the electrons appear to be heated sufficiently to make their self-collision time longer than the fast ion loss time and the plasma potential reverses. Under these conditions slow ions produced by ionization of the residual gas are trapped and a slow ion component to the plasma is built up. This increases the fast neutral atom trapping and therefore a higher fast ion density is obtained. Under these conditions, the second and third harmonic emission is suppressed and there is some first harmonic emission; but less than when the resonance zone is 10% above the bottom of the well. In this condition the energy spreading is also less.

Fig.15 shows some of this behaviour. In this particular case the magnetic field was ramped through the electron cyclotron resonance. At the beginning of the pulse the magnetic field is too high for resonance anywhere in the well and the behaviour is normal; emission occurs at the second, third and fourth harmonics of the ion gyro-frequency. As the magnetic field is ramped down, resonance with the lowest part of the well occurs. As far as can be seen in this figure all R-F emission stops and the signal on the fast atom detector (measuring central density) rises by about a factor of two. As the field falls and the resonance zone rises in the well there is a large spillage of the trapped cold ions, emission appears in the first harmonic and the fast ion density falls again.

It is too early to assess completely the significance of these results. The suppression of the higher harmonics occurs under conditions when electron Landau damping is expected to be important, but the appearance of the strong emission at the fundamental of the ion gyro-frequency is not completely understood at the moment. Two likely explanations are:

(i) the appearance of a hot electron version of the instability[5].

or (ii) the appearance of an instability associated with the presence of cold ions[5].

## 5. ACKNOWLEDGEMENTS

The authors wish to thank J. Coupland, P. Hammond and all the members of the PHOENIX operating team without whom this work would not have been possible, and A. Cole, A.I. Kilvington, A. Steed and J.A. Turner, who provided most of the diagnostic apparatus.

## 6. REFERENCES


1. BERNSTEIN, W., CHECHKIN, V.V., KUO-PETRAVIC, L.G., MURPHY, E.G., PETRAVIC, M., RIVIERE, A.C. and SWEETMAN, D.R. Plasma produced by neutral injection into a magnetic mirror/well geometry. Plasma Physics and Controlled Nuclear Fusion Research, Conference Proceedings, vol.II, pp.23-44, Vienna, IAEA, 1966.

2. HARRIS, E.G. Plasma instabilities associated with anisotropic velocity distribution. Journal of Nuclear Energy, (Pt.C) - Plasma Physics, vol.2, January 1961, pp.138-145.

3. BEASLEY, C.O. and CORDEY, J.G. Convective and absolute ion cyclotron instabilities in homogeneous plasmas. Plasma Physics, vol.10, no.4, April 1968, pp.411-419.

4. KUO-PETRAVIC, L.G., MURPHY, E.G., PETRAVIC, M., SINCLAIR, R.M., SWEETMAN, D.R. and THOMPSON, E. Energy spreading and stabilization of plasma by applying a high-frequency electric field, vol.7, no.1, May 1967, pp.25-27.

5. HALL, L.S., HECKROTTE, W. and KAMMASH, T. Ion cyclotron electrostatic instabilities. vol.139, no.4A, 16 August 1965, pp.A1117-A1137.

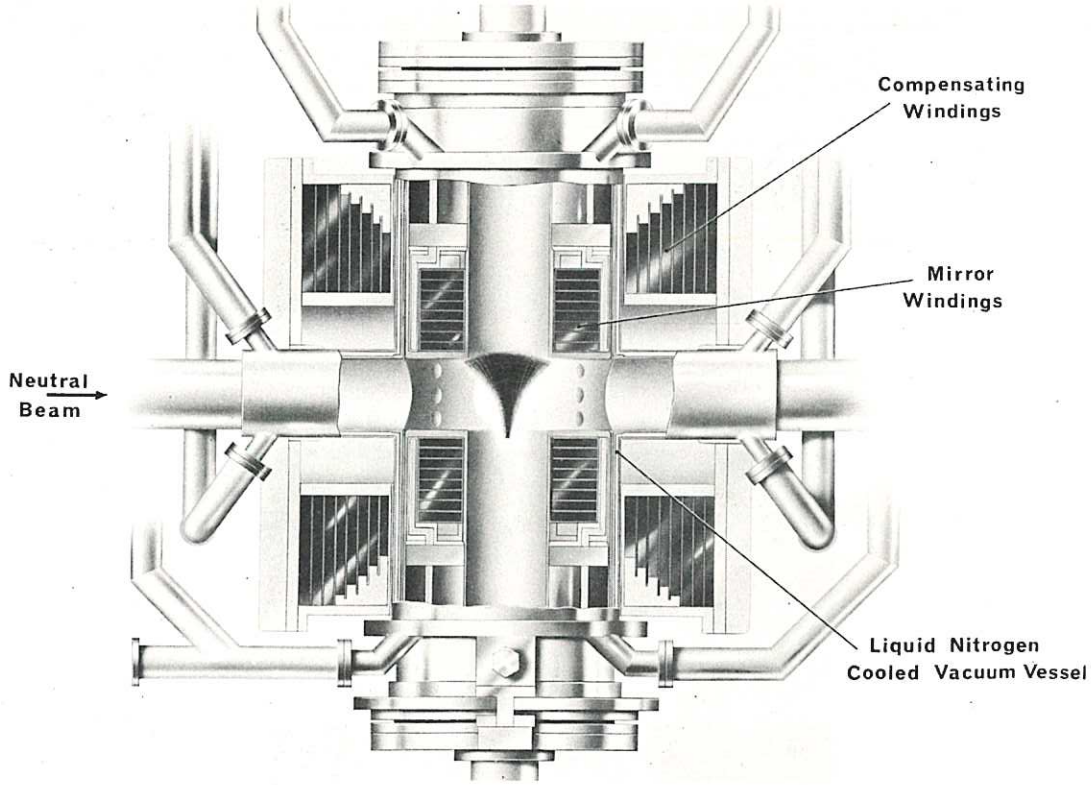


Fig. 1 Mirror and quadrupole coil structure (CLM-P174)

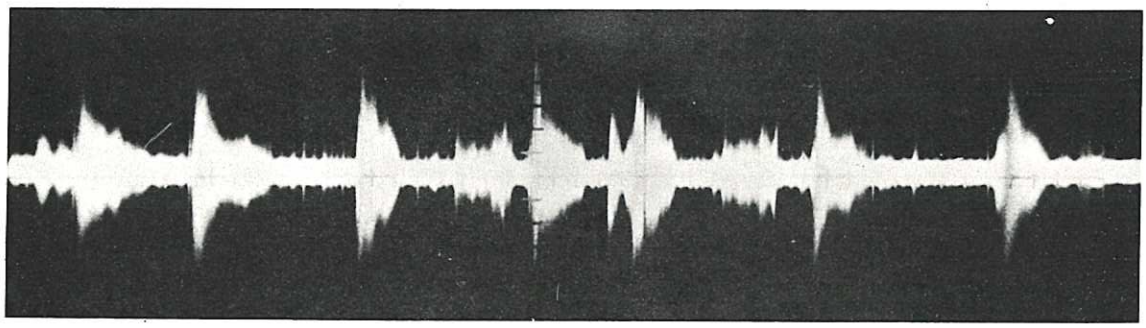


Fig. 2 R–F signal received on a loop antenna (CLM-P174)

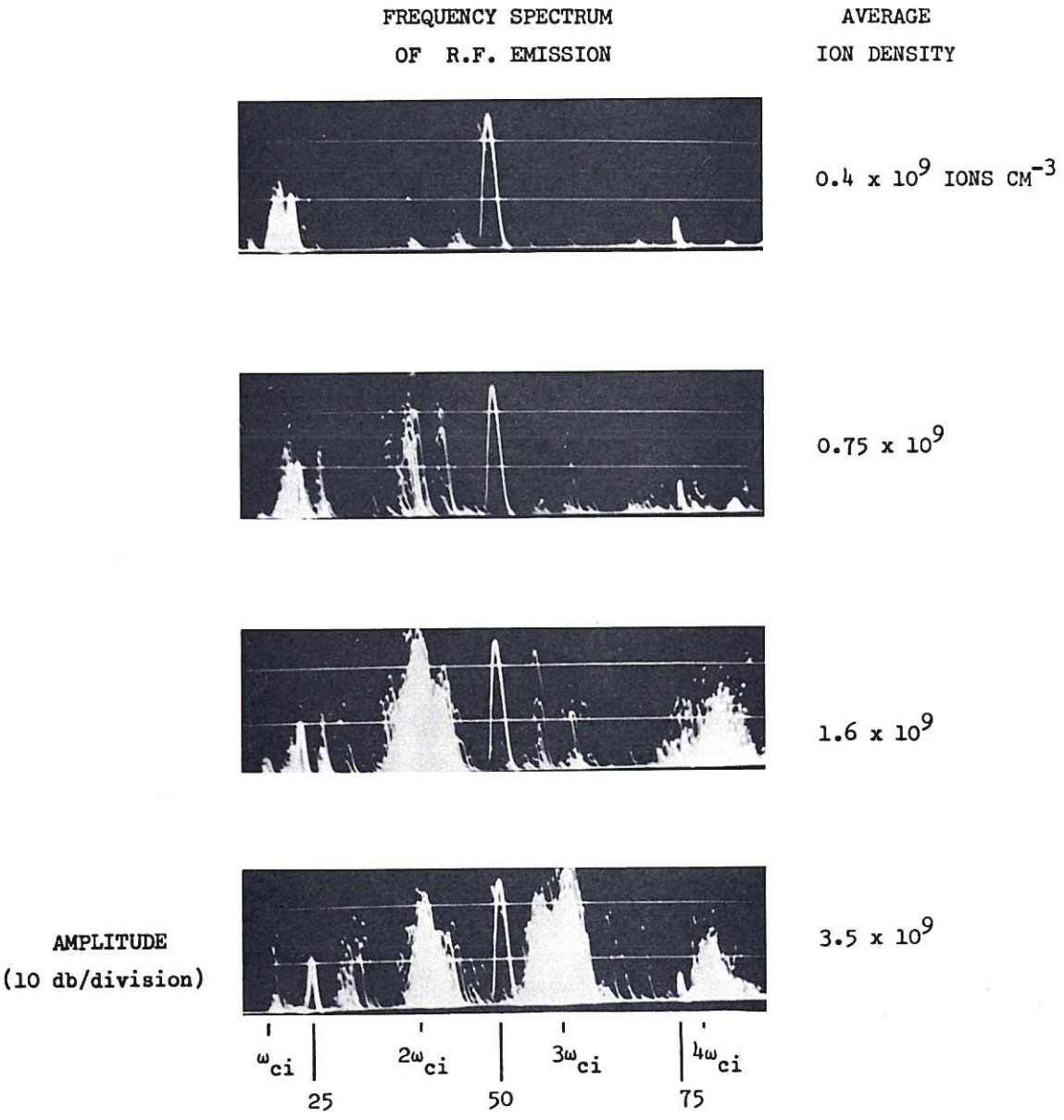


Fig. 3 (CLM-P174)

Spectra of R–F activity received on a loop aerial oriented to pick-up axial plasma currents. Spectra are swept at 500 Hz and superimposed for approximately 1 second

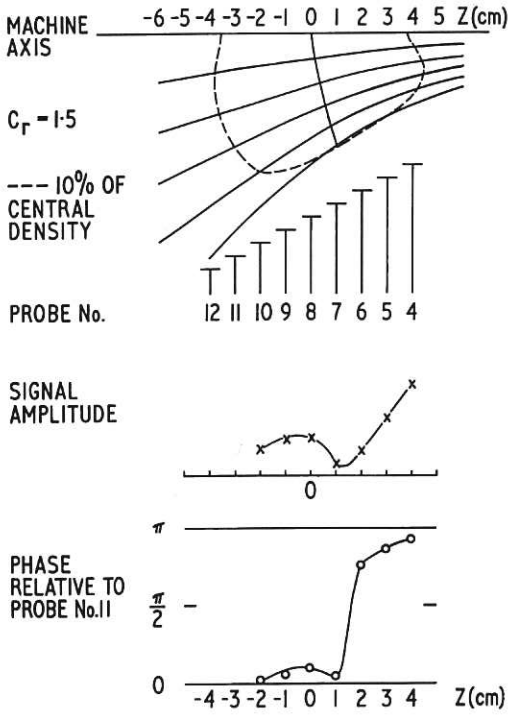


Fig. 4 (CLM-P 174)

Determination of parallel wavelength. Positioning of probes relative to plasma is indicated in the upper part of the figure, and the relative amplitude and phase in the lower part

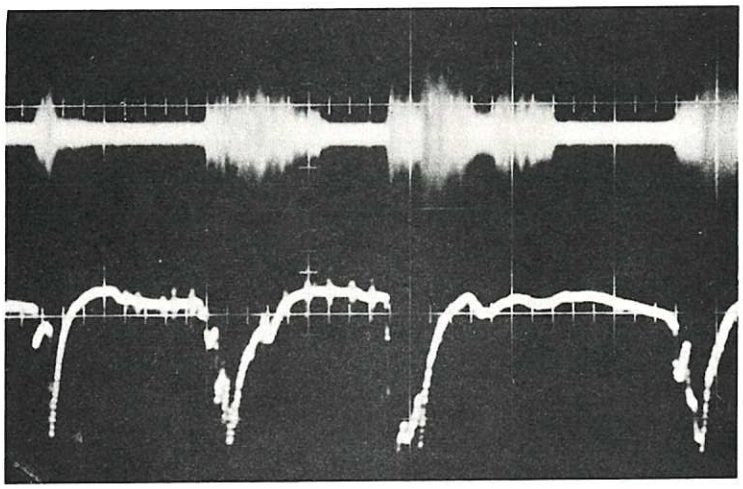


Fig. 5 (CLM-P 174)

Correlation of electron emission along field lines with R–F activity picked up on a loop aerial

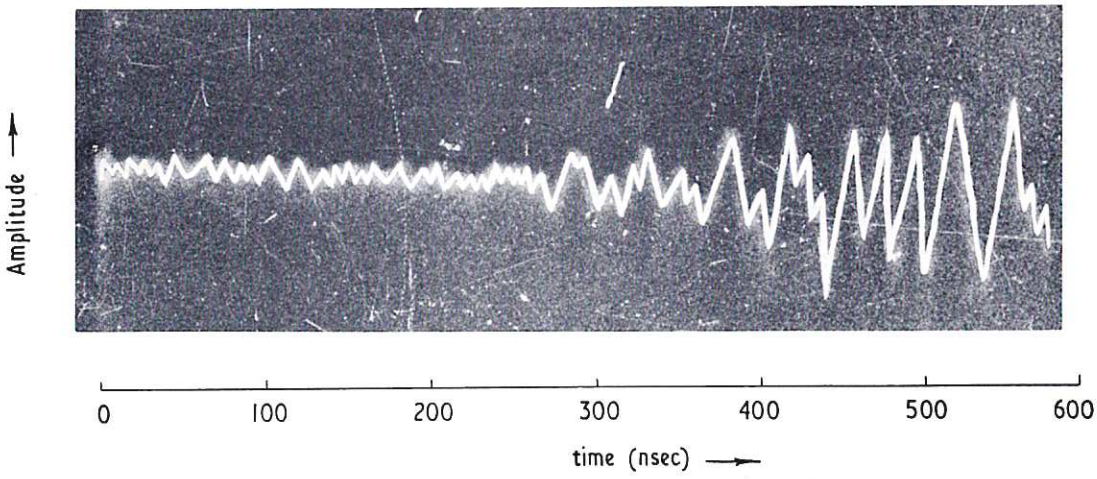


Fig. 6 (CLM-P 174)
Growth of an instability at the second harmonic of $\omega_{ci}$

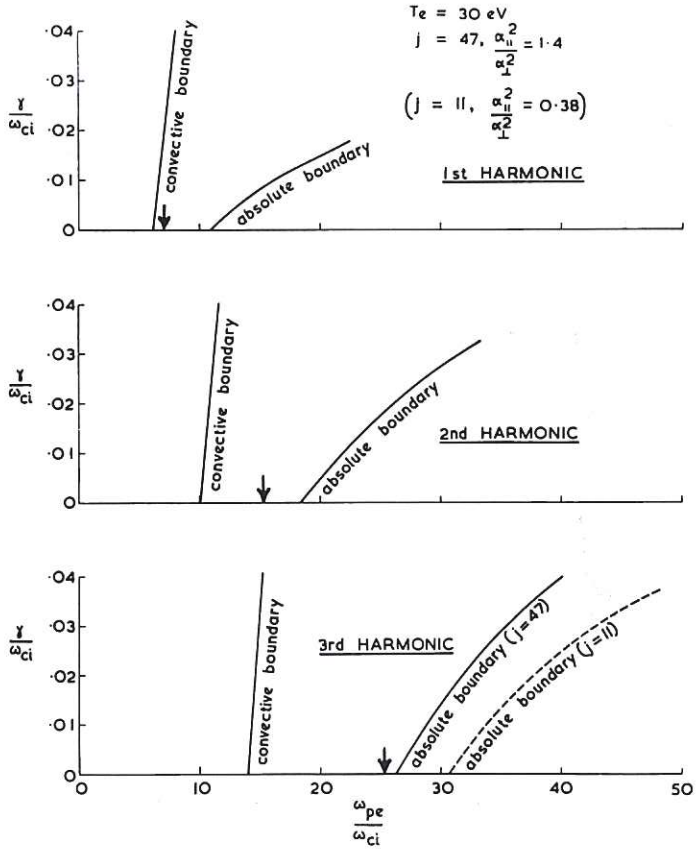


Fig. 7 (CLM-P 174)
Comparison of experimental thresholds (arrows) with growth rate computations

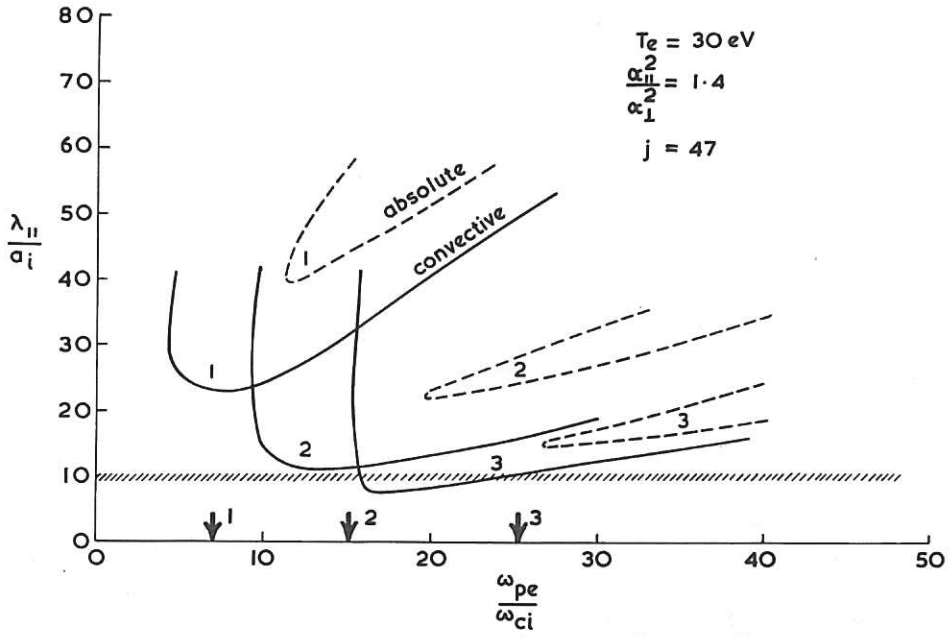


Fig. 8 (CLM-P 174)
Parallel wavelength as a function of plasma frequency for the first three harmonics of the ion cyclotron frequency

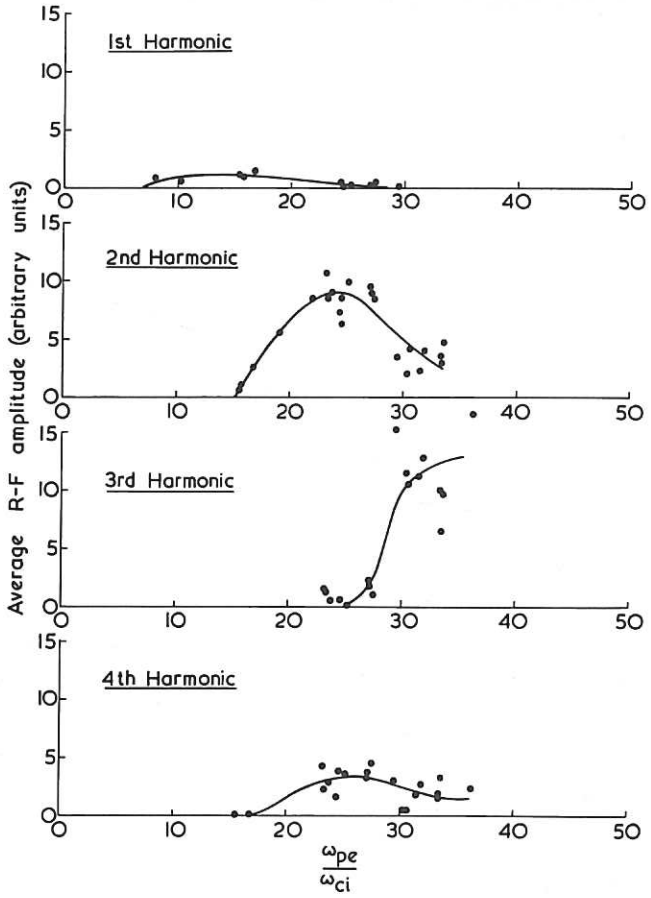


Fig. 9 (CLM-P 174)
Average amplitude of the signals at harmonics of the ion cyclotron frequency as a function of plasma frequency in PHOENIX II

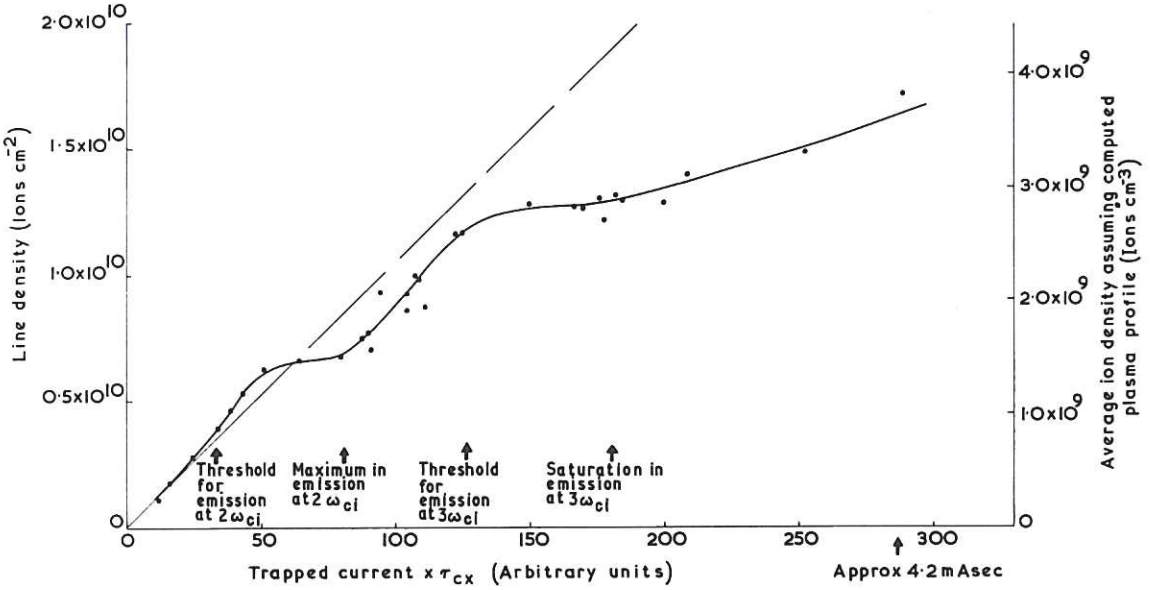


Fig. 10 (CLM-P 174)
Correlation of central line density with thresholds of r.f. emission

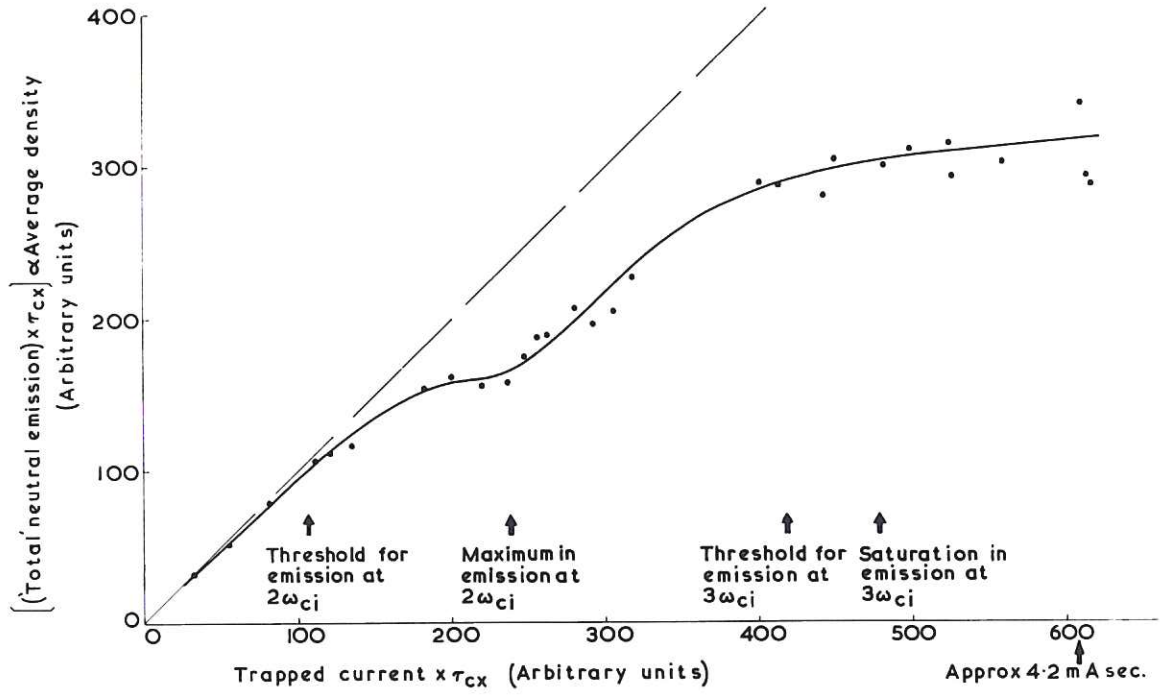


Fig. 11 (CLM-P 174)
Correlation of average ion density with thresholds for r.f. emission

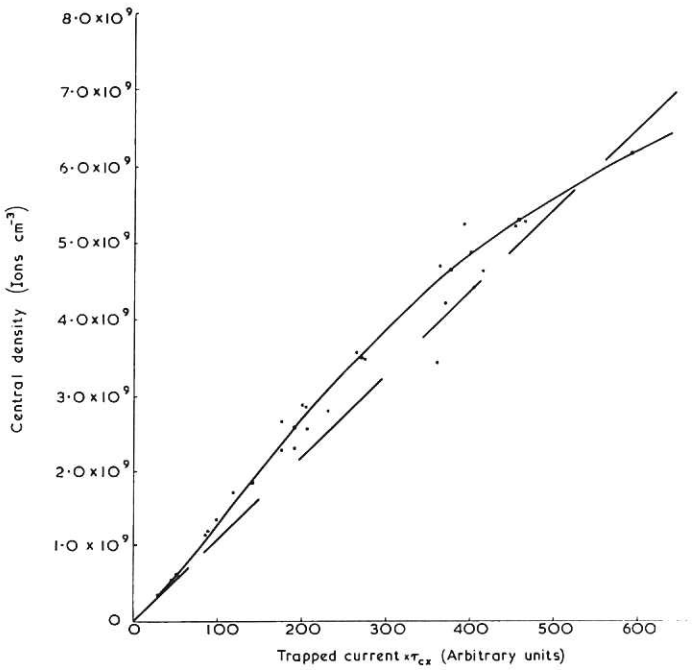


Fig. 12 (CLM-P 174)
Central ion density as a function of $I_o \tau_{cx}$

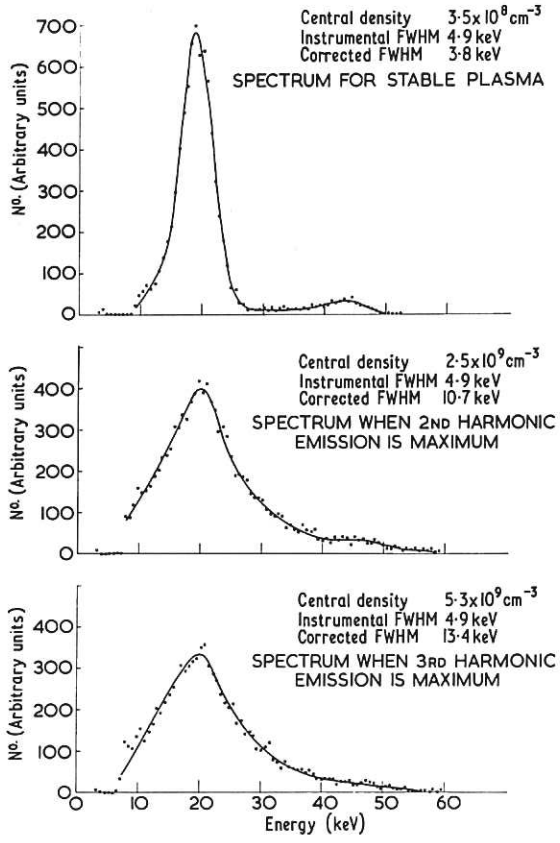


Fig. 13 (CLM-P 174)
Proton energy spectra in the median plane of PHOENIX I

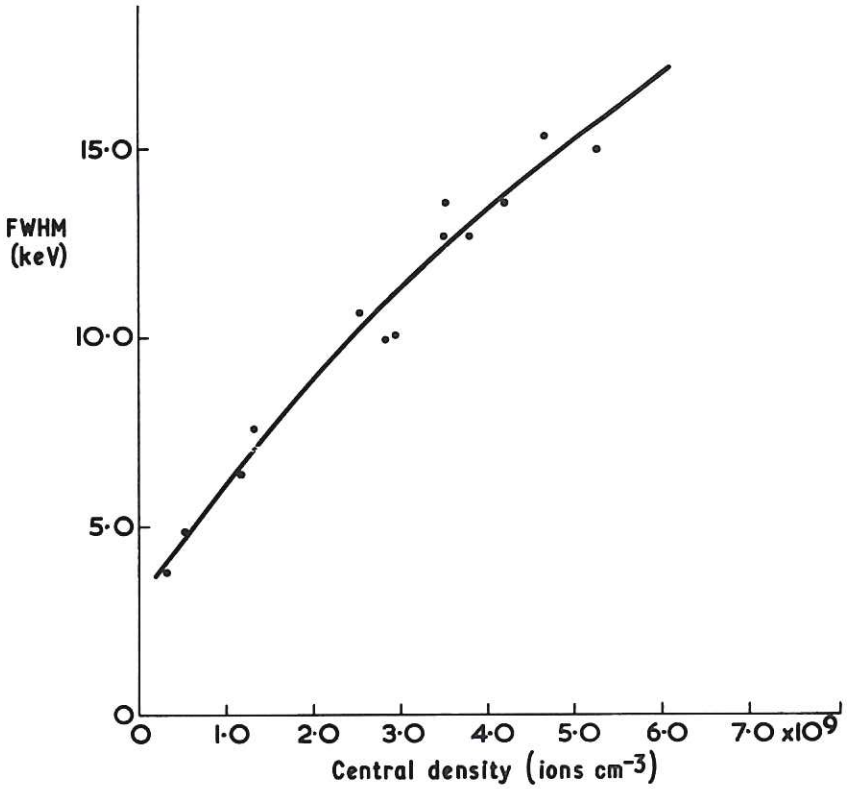


Fig. 14 (CLM-P 174)
Width of ion energy spectrum (corrected for detector resolution) as a function of a central density

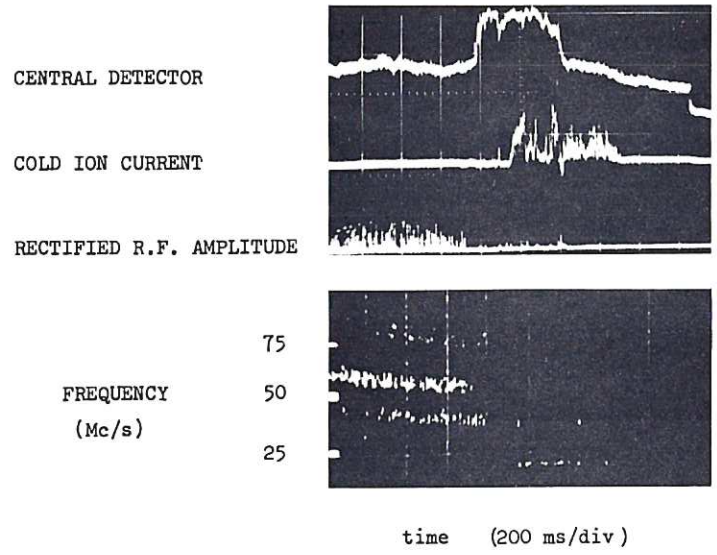


Fig. 15 (CLM-P 174)
Effect of microwave heating. The magnetic field is ramped downwards through the cyclotron resonance. See text for detailed discussion